

## Coupled MBS-CFD Simulation of the IDEOL Floating Offshore Wind Turbine Foundation Compared to Wave Tank Model Test Data

Friedemann Beyer<sup>1</sup>, Thomas Choynet<sup>2</sup>, Matthias Kretschmer<sup>1</sup>, Po Wen Cheng<sup>1</sup>

<sup>1</sup>Stuttgart Wind Energy (SWE), University of Stuttgart  
Stuttgart, Germany

<sup>2</sup>IDEOL  
La Ciotat, France

### ABSTRACT

A two MW floating offshore wind turbine is currently developed within the EU-FP7 project FLOATGEN. A wave tank test of the floater model at 1/32<sup>th</sup> scale has been performed in extreme wave conditions. In the present study numerical calculations of the floating foundation with regular waves using coupled MBS-CFD methods are compared to experimental data enabling a validation. Results of the wave elevation, floater motion and mooring line tension show a very good correlation. Flow phenomena like vortex shedding at the hull of the floater are shown. The presented methodology provides detailed knowledge allowing analysis of wave impact and resulting load assessment of floating offshore structures.

**KEY WORDS:** Floating offshore wind turbine; Wave tank model test; Computational fluid dynamics; Multibody system; Numerical wave tank (NWT); Vortex shedding; Mooring line

### INTRODUCTION

The potential for floating offshore wind energy in Europe is immense and already the North Sea could meet today's EU electricity consumption by multiple times. The European Wind Energy Association (EWEA) states based on research of the EU-FP7 project ORECCA (2012) that two thirds of the North Sea have water depths between 50 m and 220 m which could be used to install floating offshore wind turbines (Arapogianni, 2013). Recently, the EU-FP7 project FLOATGEN has been kicked off to demonstrate and benchmark a floating wind turbine system for power generation in the Atlantic Ocean. The FLOATGEN demo project will deploy a two MW floating offshore wind turbine (see Fig. 1) at the SEM-REV test site located twelve nautical miles from the French Atlantic coast (FLOATGEN, 2014). SEM-REV is operated by École Centrale de Nantes, owner of the test site. Ebenhoch (2015) finds that the estimated target Levelized Cost of Energy (LCOE) for floating concepts which includes all capital-, operational- and decommissioning expenditure over the project lifetime is around 15.2 Eurocent per kWh. EWEA (Arapogianni, 2013) recommends further development and validation of numerical simulation tools to optimise and improve the design of

floating turbines to be more competitive compared to fixed-bottom concepts with a LCOE of 13.5 Eurocent per kWh (Ebenhoch, 2015).

The environmental conditions of a floating wind turbine system are dominated by turbulent winds, non-linear waves and currents. The floating structure affected by the wind turbine controller interacts with the surrounding fluids leading to induced motions, loads and deformations. For design optimisation realistic and detailed load estimates are needed. Hydrodynamics of offshore structures are commonly modelled in numerical codes using Morison equation, a semi-empiric approach, and potential flow theory. However, simple methods are not capable of including all effects as flow physics are often non-linear and highly complex. Matha (2011) explains limitations of the above mentioned hydrodynamics modelling techniques. Especially non-slender and non-cylindrical floating foundations like IDEOL's ring-shaped concept (see Fig. 1) modelled in this paper require the consideration of wave diffraction, added-mass and radiation damping (Choynet, 2014). These effects are inherently included in a Computational Fluid Dynamics (CFD) approach.



Fig. 1: Illustration of the two MW floating offshore wind turbine system within EU-FP7 project FLOATGEN (source: IDEOL)

### Literature Study

Only limited analyses on loads and dynamics of floating offshore wind turbines using CFD modelling techniques have been published in the

past. A floating wind turbine system based on a spar-buoy floater that experiences a free-decay motion in still water has been analysed by Beyer (2013) using a coupled Multibody System (MBS) and CFD methodology. Numerical simulations are compared with a MBS model applying a potential flow solver for computation of linear hydrodynamic loads. Results show the shedding of three-dimensional vortices along the structure and the influence on the pitch motion of the floater. Differences in the estimated viscous drag between both methods are discussed. Further goes Quallen (2014) by modelling both the aerodynamics and hydrodynamics of a five MW offshore wind turbine mounted to a spar-buoy floater in a single URANS CFD solver using 5.75 million points in the computational domain. A validation is presented against experimental data for free-decay tests and results show frequency differences in surge. Full-system simulations are conducted using a quasi-static crowfoot mooring line model with steady winds and waves and less floater motions are predicted compared to FAST (Jonkman, 2005) based on Blade Element Momentum (BEM) theory and linear hydrodynamics. A code-to-code comparison is shown by Benitz (2014) for the OC4 DeepCwind semi-submersible (Robertson, 2012) without wind turbine between CFD calculations based on OpenFOAM and hydrodynamic loads via potential flow theory and Morison equation. Current-only and wave-only cases are simulated for a fixed structure at 1/50<sup>th</sup> model scale for three grids of approximately three million cells. Differences in load predictions are found due to transverse forces from vortex shedding and shadowing effects of downstream floater members which are inherently simulated in CFD.

The potential of CFD calculations estimating wave impact loads on support structures of fixed-bottom offshore wind turbines (monopiles) has been studied by Bredmose (2011). The Volume of Fluid (VOF) approach is applied using OpenFOAM and breaking waves are generated utilising the wave focusing method. Results show slamming pressure and wave run-up at the monopile and demonstrate wave-structure interaction. It is found that semi-empiric Morison equation only provides good load estimates on monopiles for non-breaking waves of moderate amplitude. Paulsen (2013) presents results of the impact of two-dimensional irregular waves on a fixed-bottom circular cylinder. CFD calculations using OpenFOAM are validated against experimental measurements. Both the free surface elevation and the inline force are accurately predicted using CFD. Paulsen finds that good load estimates are also achieved for moderately steep irregular waves with a Morison equation in combination with a non-linear two-dimensional potential flow solver. For near breaking waves, however, the inline force at the monopile is more accurately predicted by means of the CFD solver. A comparison of model tests at 1/12<sup>th</sup> scale and numerical simulations using the CFD solver ANSYS CFX is described by Hildebrandt (2014) for the analysis of wave breaking on a fixed-bottom offshore wind turbine structure (tripod). Hildebrandt finds a good agreement between numerical and experimental results and compares derived slamming coefficients to load calculations based on guidelines.

During the design process of offshore structures, numerical simulations are combined with tests of a scaled model in a (combined) wind and/or wave tank. The experiments are necessary for validation and tuning purposes of numerical tools and load and motion estimates. Within the EU-FP7 project INNWIND.EU (Sandner, 2015) a floating offshore wind turbine at 1/45<sup>th</sup> scale representing the five MW OC4 DeepCwind semi-submersible and at 1/60<sup>th</sup> scale representing a generic 10 MW floating wind turbine have been tested at École Centrale de Nantes. A low-Reynolds, pitch-controlled rotor is used. Free decay tests, tests with regular and irregular waves, wind, and combined wind/wave tests are performed. Mueller (2014) compares scaling methodologies and critical issues of various wave tank test campaigns of floating offshore

wind turbines. Practical recommendations for modelling and construction of scaled rotors are given.

The present study is a continuation from Beyer (2013). CFD calculations are coupled with MBS methods to gain a high fidelity insight into predominant flow phenomena. In a preliminary step a Numerical Wave Tank (NWT) is verified in CFD using a two-dimensional undisturbed wave field that is compared to results from analytical wave theories. Optimal settings for grid spacing, time step and turbulence model are determined by means of a parameter study. Numerical simulations of the IDEOL floating offshore wind turbine foundation at 1/32<sup>th</sup> scale are compared to wave tank test measurements with regular waves. Results include timeseries of floater motion, wave elevations, mooring line tension and visualisation of vortex shedding.

## METHODOLOGY

### Numerical Tools and FMBS Coupling

Numerical simulations in this research are conducted using a coupled MBS-CFD approach. Hydrodynamic loads on the floating foundation are calculated with the commercial CFD code ANSYS CFX. It uses the Finite-Volume Method (FVM) to solve the Reynolds-Averaged Navier-Stokes (RANS) equations on structured and unstructured grids. The free surface is modelled by means of the Volume of Fluid (VOF) method that computes the shape and location of the free surface on the basis of a fractional volume function. The commercial MBS solver SIMPACK is applied for modelling of the structural properties and is coupled to CFD. The bodies of the floating system characterised with mass, centre of gravity and inertia are connected by joints of various type. External forces like simple spring-damper elements or complex aerodynamic forces on rotor blades can be applied.

The MBS-CFD coupling has been developed by Arnold (2014) for the simulation of fluid-structure interaction on tidal current turbines. It is further called Fluid-Multibody Interaction (FMBS). A motivation on its application for the analysis of hydrodynamic loads on floating offshore wind turbines is presented in Beyer (2013). A validation based on submerged free-decay experiments of spring, gravity and bending pendulums in an aquarium filled with water is demonstrated by Arnold (2015). An excellent correlation between numerical and experimental results demonstrates the validity of the methodology. The challenge of the coupling methodology is the transfer of loads and motion information between the CFD and MBS solver (see Fig. 2). Essential tasks are coordinate transformation and interpolation, collection of loads and motion information and the transfer to a common storage. Also important are the distribution of loads and motion data and the synchronisation. A fully implicit iteration scheme is incorporated for transient simulations. Every time step is subdivided into multiple coefficient loops (inner iterations) and coupling data is exchanged. The MBS solver is repeated after each coupling time step integration. Convergence and the number of coefficient loops of each time step are controlled by a moderator via user input.

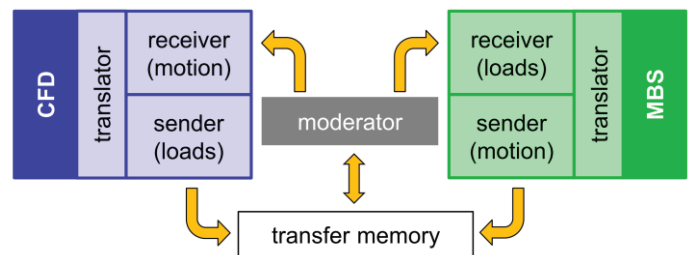


Fig. 2: Structure of the MBS-CFD coupling

## Wave Tank Model Test

Within the project FLOATGEN a model test campaign has been performed by OCEANIDE in its offshore basin BGO FIRST at La Seyne Sur Mer in France (see Fig. 3).

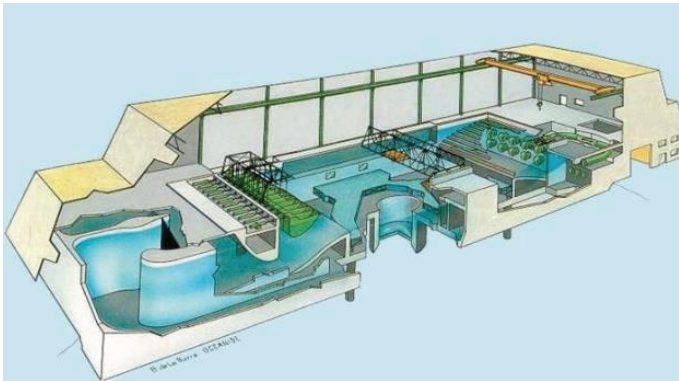


Fig. 3: Offshore basin BGO FIRST at La Seyne Sur Mer (source: OCEANIDE)

Objectives of the campaign are to test the mooring system and the dynamic behaviour of the IDEOL floating offshore wind turbine foundation in extreme wave conditions and shallow depth. Froude similitude is applied and a mock-up of the floater at  $1/32^{\text{th}}$  scale is tested. A simplified wind turbine model is used by representing the tower by a steel pipe and the Rotor-Nacelle Assembly (RNA) by a lumped mass at the tower top. The mooring system is represented by three steel cables that are connected to springs. Free decay tests, tests with regular and irregular waves and currents are performed without winds. Measurements used in this study include six Degrees-of-Freedom (DOF) floater motion, wave elevations at multiple locations around the floater, green water forces on two containers on the deck and the axial tension of the mooring lines at the fairleads (see Fig. 4).

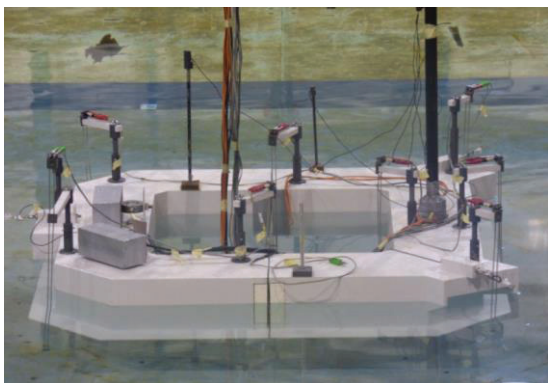


Fig. 4: Test mock-up of the IDEOL floating offshore wind turbine foundation at  $1/32^{\text{th}}$  scale with instrumentation (source: IDEOL)

## COMPUTATIONAL MODEL

### Numerical Wave Tank

#### Mesh and Boundary Conditions

For reasons of simplification only the floater surge, heave and pitch motion are enabled. Thus, a symmetry plane is used and the domain is cut in half. The three-dimensional computational domain is discretized into a structured grid using ICM CFD with 1.2 million hexahedra

elements (see Fig. 5). A structured mesh provides a better flow quality and scaling of the CPU-power, but is more time consuming in generating than unstructured meshes. An O-grid (grid lines are arranged like an “O” shape to reduce skew (Ansys, 2014)) is used around the floater and the grid is refined close to the hull of the floater to resolve the boundary layer. The floater mesh is simplified without inclusion of the containers at the fore used for measuring of green water loads, the tower at the aft and the mooring interface structure. The rigid floater is modelled using a no-slip wall boundary condition. The seabed and sidewall are represented by free-slip walls. The top boundary of the NWT is of type opening with static pressure option while the outlet has a specified relative pressure based on the hydrostatic pressure distribution. An opening is defined at the inlet with specified velocity components  $u$  and  $w$  and volume fraction of air and water. Parallel to boundary mesh motion is used for the seabed, sidewall and top boundary while a specified displacement is set for the fluid domain and floater. The mesh is deformed in the vicinity of the floating foundation based on its motion. The NWT is approximately four wavelengths long ( $x$ ), one wavelength wide (half field,  $y$ ) and two wavelengths deep ( $z$ ).

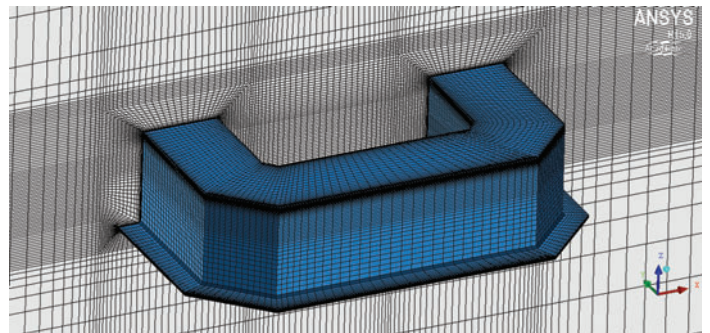


Fig. 5: Illustration of the surface mesh of the floating foundation

### Wave Generation and Damping

A wave generator has been developed within the CFD tool as it is not included as a standard feature. The implementation of the so called WAVES2CFX function is based on a user CFX Expression Language (CEL) function written in Fortran (see Fig. 6). It is interfaced with the user CFX Command Language (CCL) that enables the user to specify parameters like wave theory, (significant) wave height and period, water depth etc. Using location and time information the WAVES2CFX function computes velocity, pressure and wave elevation for regular/irregular linear (Airy) and Fenton wave theory. An expression is used to compute the wave elevation and resulting volume fraction of air and water by calling WAVES2CFX. The Cartesian velocity components  $u$  and  $w$  are also calculated by WAVES2CFX.

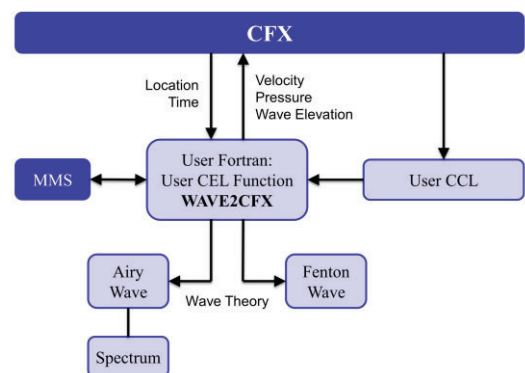


Fig. 6: Implementation scheme of wave generator WAVES2CFX

A numerical beach is used to damp out waves behind the measuring zone and to avoid reflections. It is implemented by means of momentum source terms  $S_x$  and  $S_z$  in  $x$ - and  $z$ -direction acting on the computational domain (see Fig. 7). Additionally, numerical damping is enforced in the beach with cells of increasing size.

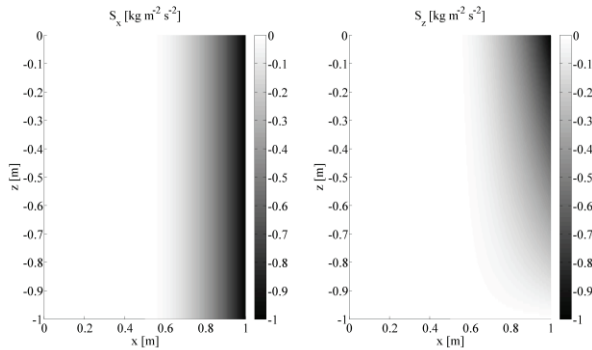


Fig. 7: Illustration of the momentum source terms  $S_x$  and  $S_z$  used for modelling of the numerical beach (here  $0.5 \text{ m} \leq x \leq 1.0 \text{ m}$ )

### Time Advection and Partitioning

A homogeneous multiphase fluid model is used. Thus, all fluids share the same velocity and turbulence field. The SST turbulence model (Menter, 1994) with curvature correction and Kato Launder production limiter (Ansys, 2014) is applied. The two-equation eddy-viscosity model combines the  $k-\omega$  model in the viscous boundary layer and the  $k-\varepsilon$  model in the free-stream.

A first order backward Euler transient scheme is applied with first order turbulence numerics option. The time step is fixed in the FMBI simulation. A parameters study of, amongst other things, the time step in a two-dimensional wave tank without the floater has been conducted. Taking into account the accuracy, stability and efficiency of the simulation  $dt$  is set to  $1/35^{\text{th}}$  of the wave period  $T$ . The implicit solver scheme is divided into three inner iterations enabling convergence and robustness.

The CFD simulation is run in parallel for reduction of duration. Thus, the computational domain is divided in several subdomains during the partitioning and each is associated to a solver process. However, CFD simulations with a free surface are not robust if a portion of a partition boundary is parallel to the free surface (Ansys, 2014). A user specified partitioning method with division in the  $x$ -direction (direction of wave propagation) is found to be most stable (see Fig. 8). Though, the partition boundaries are perpendicular to the free surface. But the water runs over the deck of the floating foundation and downwards at the aft during the simulation (see red circle in Fig. 8). As a result some parts of the free surface are aligned with a partition boundary and the simulation becomes unstable. To resolve this issue a user specified partition weighting is used to shift the partition boundaries away from potential locations with aligned free surface.

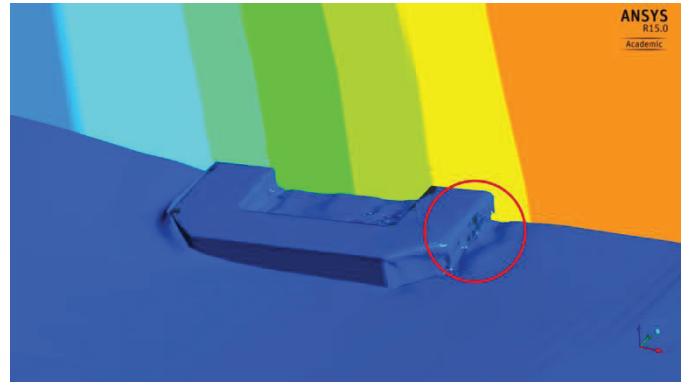


Fig. 8: User specified partitioning of the domain (coloured planes) in a parallel CFD run; red circle indicates a potential region of the free surface that is parallel to a partition boundary

### Structural Model

The structural model is specified in the MBS tool by mass, centre of gravity and moments of inertia of the rigid floater, tower and RNA. Three floater DOFs are enabled - surge, heave and pitch motion. Hydrodynamic loads and floater motion information are exchanged via a user force element called CFX2SPCK. The mooring system is modelled by three springs that are calibrated to the global linear stiffness of the mooring lines used in the wave tank model tests. Results of the restoring force over the displacement in  $x$ -direction (surge) are shown in Fig. 9.

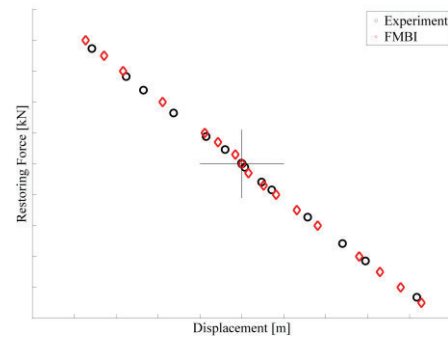


Fig. 9: Calibration of the mooring system showing the restoring force over the displacement in  $x$ -direction (surge) with reference marker at zero values

## RESULTS AND DISCUSSION

### Load Case Selection

In the wave tank model test campaign the behaviour of the floating foundation is investigated with respect to extreme wave conditions. A selection of load cases used for the analysis with the FMBI simulations is based on extreme values for the green water load sensors and relative wave elevation sensors. Here only one test case with regular waves of wave height  $H = 6 \text{ m}$  and period  $T = 10 \text{ s}$  is analysed.

### Wave Elevation

Wave calibration is done in the wave tank for each test case without the model of the floating foundation. Wave probes are located at several locations in the basin. Similar environmental conditions have to be

reproduced in the numerical simulation. The most important parameter is the wave height and velocity at the floating foundation. Thus, a two-dimensional NWT is used to calibrate the input parameters of the wave generator WAVES2CFX. As the numerical damping of the wave elevation along the direction of the wave propagation is almost linear, a linear scaling factor is applied for calibration. A comparison of the wave elevation after transients at a plane located  $1/3^{\text{rd}}$  of the wave length in front of the floater zero position and experimental data of the wave calibration at the floater zero position is shown in Fig. 10. A good correlation of maximum amplitudes and wave period is achieved. However, the propagating wave in CFD is affected by numerical damping. Thus, the wave elevation at the floater mean position is slightly smaller compared to measurements. A reference probe measuring the total wave field during the wave tank tests with the model in the basin is not used for wave calibration of the numerical wave generator as the wave field is influenced by wave radiation of the floater.

A ramp function is used for the wave elevation to reduce numerical errors at the beginning of the simulation (Senturk, 2011). Starting from the still water surface at initialisation the waves are increased gradually.

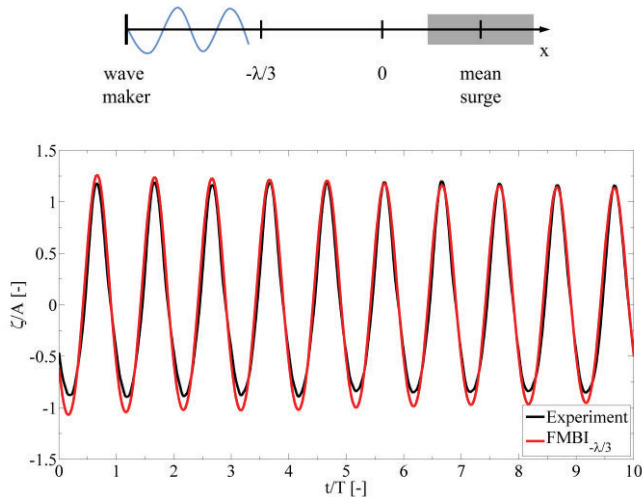


Fig. 10: Comparison of the non-dimensional wave elevation at a plane located  $1/3^{\text{rd}}$  of the wave length in front of the floater and experimental wave calibration data

### Floater Motion

The floater motion is influenced by several parameters. A correlation between numerical and experimental results is expected if the environmental conditions (waves), external forces (mooring system) and floater structural properties and geometry are modelled similarly. CFD solver settings play another important role. A comparison of the floater DOFs surge, heave and pitch is demonstrated in Fig. 11. Experimental data of ten wave periods after transients is extracted and the phase of the FMBI results is shifted to match with the measurements. The results are non-dimensional with respect to the experimental data.

The initial position of the floating foundation in the FMBI is at  $x = y = z = 0$ . Drift loads acting on the floater interact with the mooring system and lead to a mean surge position  $x_{mean}$  that is reached in the simulation after approximately 15 periods. The transient phase is included in Fig. 11. The surge response shows a very good correlation between numerical and experimental results. The period is matched and the mean and extreme values are quite similar after transients indicating a good reproduction of the conditions in the wave tank model test.

However, the transient phase is still ongoing after  $t/T = 10$  and longer simulations are needed. Transients of the heave motion are even less than for surge indicating strong floater heave damping. An excellent correlation is achieved with similar periods, minimum and maximum amplitudes and mean position. However, deviations occur for the floater pitch motion with smaller mean, maximum and minimum values of the FMBI simulation. This can be explained by simplifications of the floater geometry in the CFD model, especially the mooring interface structure at the front of the hull and the non-symmetrical arrangement of containers on the deck should induce motions in the wave tank model test. Additional, the wave elevation at the floater mean position is a little smaller compared to measurements (see discussion above). Thus, the amount of green water on deck is less than in the experiment. Floater sway, roll and yaw DOF are deactivated in the simulation leading to further differences between numerical modelling and wave tank model test.

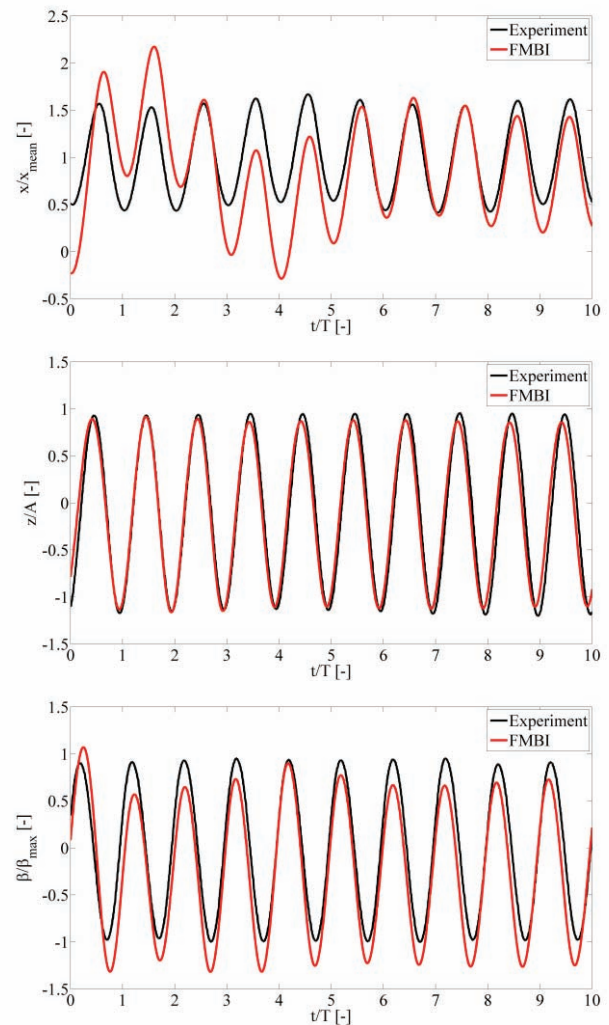


Fig. 11: Non-dimensional floater motion over simulation time for experimental and numerical results, top: surge ( $x$ ), middle: heave ( $z$ ), bottom: pitch ( $\beta$ ) motion

### Mooring Line Tension

Mooring line tensions correlate with the floater motion. Thus, the non-dimensional tension of mooring line 1 at the front of the floater agrees well with the experiment after transients similar to the floater surge

motion (see Fig. 12). The transient phase is included in Fig. 12 and is still ongoing after  $t/T = 10$  indicating the need for longer simulations. As the mooring system is modelled in MBS the good correlation is an indication for a well-functioning coupling between MBS and CFD.

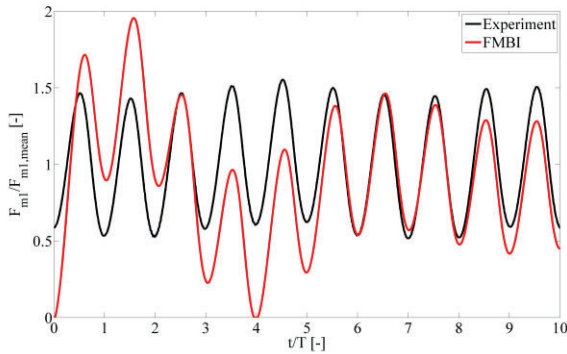


Fig. 12: Non-dimensional mooring line tension (line 1 at the front) over simulation time for experimental and numerical results

### Heave Damping and Vortex Shedding

The floating foundation experiences complex flow phenomena. The IDEOL floating offshore wind turbine foundation has strong heave damping due to the entrapped water in the damping pool<sup>®</sup>. While the floater is moving water flows in and out of the pool similar to a piston in an engine resulting in induced viscous drag. Wave sloshing can be observed in the pool. Also the water level in the pool is different compared to the wave elevation in front of the floating foundation. The deck of the floater is flooded due to large waves. Entrapped air bubbles on deck occur and the green water is flowing into the pool. The floater motion due to incident waves induces large vortices that are shed at the skirt and inner hull of the floater as demonstrated in Fig. 13 for advancing time step.

The resulting fluid-structure interaction leads to heave damping. The  $q$ -criterion is used for visualisation of vortex shedding and is based on the computation of the second invariant of the velocity gradient tensor (Ansys, 2014). In Fig. 13 the floater first is at the maximum heave position and then moves for- and downward as can be seen by the reference marker at mean surge and zero heave position. After reaching the minimum heave position in the third figure the floater moves back- and upward due to the incoming wave.

Numerical simulation of wave sloshing is challenging and results are currently compared with respect to measurements of relative wave elevation sensors located in the damping pool<sup>®</sup> of the floater and video recordings of the wave tank model tests. However, results of the global motion of the floating foundation show a good correlation between numerical and experimental results indicating a sufficient capture of predominant flow effects and temporal discretisation.

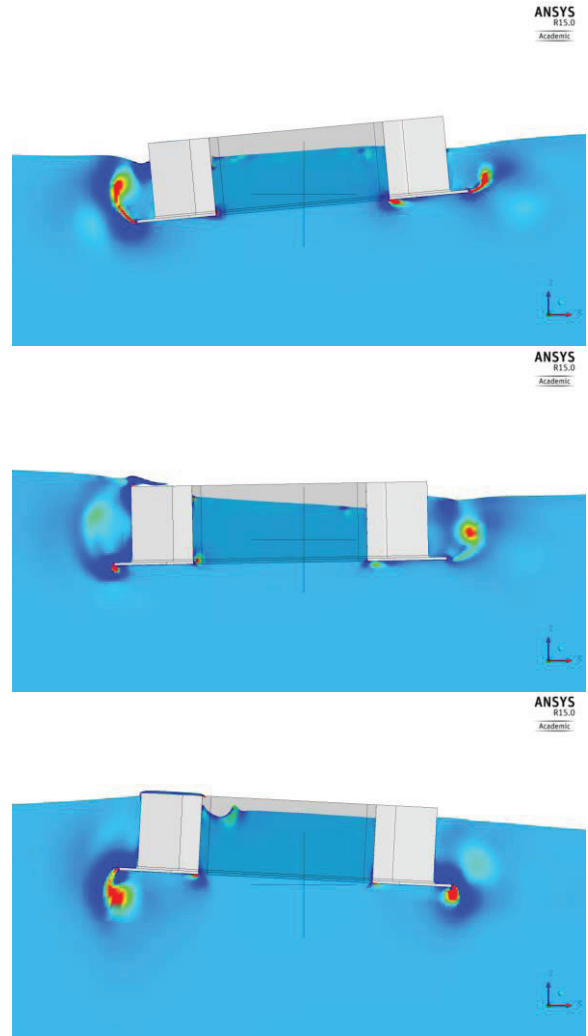
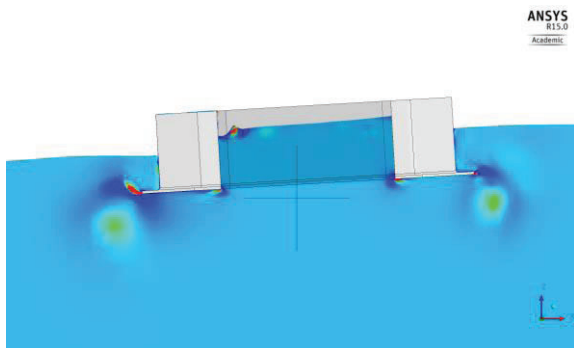
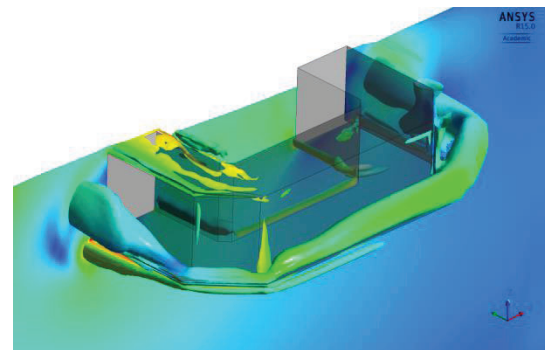


Fig. 13:  $xz$ -plane ( $y = 0$ ) illustrating vortex shedding at the floating foundation using the  $q$ -criterion; reference marker is located at  $x/x_{mean} = 1$  and  $z = 0$ ; from top to bottom: advancing time step  $t/T = 8.5$ ,  $t/T = 8.8$ ,  $t/T = 9.0$ ,  $t/T = 9.2$

The shed vortices around the floating foundation are strongly three-dimensional as shown in Fig. 14. This flow phenomenon can only be captured by high fidelity CFD simulations.



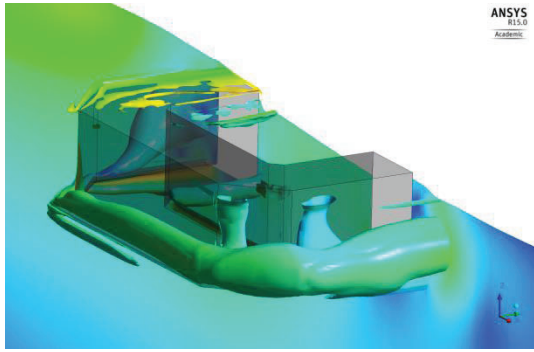


Fig. 14: Isometric view illustrating three-dimensional vortex shedding around the floating foundation using the  $q$ -criterion; colouring: magnitude of water velocity;  $t/T = 9.0$

## CONCLUSIONS

Within this study a coupling between MBS and CFD is successfully applied to the simulation of wave impact on a floating offshore wind turbine foundation. A wave tank test of the floater model at  $1/32^{\text{th}}$  scale has been performed in extreme wave conditions within the EU-FP7 project FLOATGEN. A numerical wave tank is setup in CFD and wave generation and damping is tested. A regular wave test case with extreme values for green water loads and relative wave elevation is selected. A calibration of the wave elevation is presented. Floater motion in surge, heave and pitch and mooring line tension show a very good correlation after transients between numerical and experimental results. The floater experiences strong heave damping that is caused by vortex shedding at the hull of the floater and the moving water in the pool. Using nine solver processes and the presented solver settings the simulation time is approximately 1.5 hours per wave period. The presented methodology provides very satisfactory results and may be used for load assessment and design optimisation of various types of offshore structures.

In the near future the presented simplifications of the CFD mesh shall be eliminated enabling analysis of green water loads on the containers. Furthermore, experimental data of relative wave elevation sensors located around the floater may be analysed for estimation of wave run-up at the tower. After simulation of the floater at  $1/32^{\text{th}}$  scale a six DOF full scale model shall be simulated and analysed.

## ACKNOWLEDGEMENTS

The presented work is funded partially by Voith Hydro Ocean Current Technologies GmbH & Co. KG and the European Community's Seventh Framework Programme (FP7) under grant agreement number 295977 (FLOATGEN). The presented work is supported by Simpact AG and Ansys Germany GmbH. I would like to acknowledge IDEOL for graciously supplying the wave tank model test data. S.D.G.

## REFERENCES

ANSYS Inc. (2014). "ANSYS 15.0 Theory Manual".  
 Arapogianni A, Genachte AB (2013). "Deep Water - The next Step for Offshore Wind Energy," *Report by the European Wind Energy Association*, July 2013.  
 Arnold M, Cheng PW, Biskup F (2014). "Simulation of Fluid-Structure-Interaction on Tidal Current Turbines Based on Coupled Multibody and CFD Methods," *Journal of Ocean and Wind Energy*, ISOPE, Vol. 1, No. 2, May 2014, pp. 119–126.

Arnold M, Kretschmer M, Koch J, Cheng PW (2015). "A Validation Method For Fluid-Structure-Interaction Simulations Based On Submerged Free Decay Experiments," *Proceedings of 25th International Ocean and Polar Engineering Conference*. Kona, Hawaii, ISOPE, Vol 1.  
 Benitz M, David D, Schmidt P, Lackner MA, Stewart GM, Jonkman J, Robertson A (2014). "Comparison Of Hydrodynamic Load Predictions Between Reduced Order Models And Computational Fluid Dynamics For The OC4-DeepCWind Semi-Submersible," *Proceedings of the 33rd International Conference on Ocean, Offshore and Arctic Engineering*. ASME, San Francisco, USA.  
 Beyer F, Arnold M, Cheng PW (2013). "Analysis of Floating Offshore Wind Turbine Hydrodynamics Using Coupled CFD and Multibody Methods," *Proceedings of 23rd International Ocean and Polar Engineering Conference*. Anchorage, Alaska, ISOPE, Vol 1.  
 Bredmose H, Jacobsen NG (2011). "Vertical Wave Impacts on Offshore Wind Turbine Inspection Platforms," *Proceedings of the 30th International Conference on Ocean, Offshore and Arctic Engineering*. ASME, Rotterdam, The Netherlands.  
 Choynet T, Favré M, Lyubimova M, Rogier E (2014). "A Robust Concrete Floating Wind Turbine Foundation For Worldwide Applications," *Proceedings of Grand Renewable Energy 2014 Conference, AWTEC 2014*, Tokyo, Japan.  
 Ebenhoch R, Matha D, Marathe S, Munoz PC, Molin C (2015), "Comparative Levelized Cost of Energy Analysis," *Proceedings of 12th Deep Sea Offshore Wind R&D Conference, EERA DeepWind'2015*, Trondheim, Norway.  
 FLOATGEN (2014). "Kick-off meeting for the renewed FLOATGEN project, leading the way in European deep offshore wind energy with the first floating wind turbine demo in France," Press Release, Nantes, France, June 24th 2014.  
 Hildebrandt A (2013). "Hydrodynamics of Breaking Waves on Offshore Wind Turbine Structures," *Dissertation*, Gottfried Wilhelm Leibniz Universität Hannover, 2013.  
 Jonkman J, Buhl Jr ML (2005). "FAST User's Guide," *Technical Report*, NREL/EL-500-38230, Golden, USA.  
 Matha D, Schlipf M, Pereira R (2011). "Challenges in Simulation of Aerodynamics, Hydrodynamics, and Mooring-Line Dynamics of Floating Offshore Wind Turbines," *Proceedings of 21st International Ocean and Polar Engineering Conference*, Maui, Hawaii, ISOPE, Vol 1.  
 Menter FR (1994). "Two-Equation Eddy-Viscosity Turbulence Models for Engineering Applications", *AIAA Journal*, Vol. 32, No 8., pp. 1598-1605.  
 Morison JR, O'Brien MP, Johnson JW, Schaaf SA (1950). "The force exerted by surface waves on piles", *Petroleum Transactions (American Institute of Mining Engineers)* 189: 149–154.  
 Mueller K, Sandner F, Bredmose H, Azcona J (2014). "Improved Tank Test Procedures For Scaled Floating Offshore Wind Turbines," *Proceedings of the International Wind Engineering Conference, IWEA 2014*, Hannover, Germany.  
 Paulsen BT, Bredmose H, Bingham HB, Schløer S (2013). "Steep Wave Loads From Irregular Waves on an Offshore Wind Turbine Foundation: Computation and Experiment," *Proceedings of the 32nd International Conference on Ocean, Offshore and Arctic Engineering*, ASME, Nantes, France.  
 Quallen S, Xing T, Carrica P, Li Y, Xu Jun (2013). "CFD Simulation of a Floating Offshore Wind Turbine System Using a Quasi-Static Crowfoot Mooring-Line Model," *Journal of Ocean and Wind Energy*, ISOPE, Vol. 1, No. 3, August 2014, pp. 143-152.  
 Robertson A, Jonkman J, Masciola M, Goupee A, Coulling A, Luan C (2012). "Definition of the Semisubmersible Floating System for Phase II of OC4", *Technical Report*, NREL/TP-5000-60601, Golden, USA.

Sandner F, Amann F, Azcona J, Munduate X, Bottasso CL, Campagnolo F, Robertson A (2015). "Model Building and Scaled Testing of 5MW and 10MW Semi-Submersible Floating Wind Turbines," *Proceedings of 12th Deep Sea Offshore Wind R&D Conference, EERA DeepWind'2015*, Trondheim, Norway.

Senturk U (2011). "Modeling Nonlinear Waves in a Numerical Wave Tank with Localized Meshless RBF Method." *Computers & Fluids* 44 (1) (May): 221–228.